Kinetic versus ideal magnetohydrodynamic modelling of the resistive wall mode in a reversed field pinch plasma

M. Mulec, I. B. Ivanov, M. F. Heyn, and W. Kernbichler

Citation: Phys. Plasmas **19**, 032502 (2012); doi: 10.1063/1.3691653
View online: http://dx.doi.org/10.1063/1.3691653
View Table of Contents: http://pop.aip.org/resource/1/PHPAEN/v19/i3
Published by the American Institute of Physics.

Kinetic versus ideal magnetohydrodynamic modelling of the resistive wall mode in a reversed field pinch plasma

M. Mulec,[1] I. B. Ivanov,[1,2] M. F. Heyn,[1] and W. Kernbichler[1]
[1]*Institut für Theoretische Physik - Computational Physics, Technische Universität Graz, Association EURATOM-OEAW, A–8010 Graz, Austria*
[2]*Petersburg Nuclear Physics Institute, 188300, Gatchina, Leningrad Region, Russia*

(Received 23 August 2011; accepted 17 January 2012; published online 9 March 2012)

Resistive wall modes (RWMs) are studied within the kinetic model proposed by Heyn *et al.* [Nucl. Fusion **46**, S159 (2006); Phys. Plasmas **18**, 022501 (2011)], which accounts for Landau damping, transit-time magnetic pumping, and Coulomb collisions in cylindrical geometry. Results for the reversed field pinch plasma are compared to the magnetohydrodynamic results obtained by Guo *et al.*, [Phys. Plasmas **6**, 3868 (1999)]. Stabilization of the external kink mode by an ideal wall as well as stabilization of the resistive wall mode by toroidal plasma rotation is obtained. In contrast to MHD modelling, which predicts a stability window for the resistive wall position, kinetic modelling predicts a one sided window only, i.e., the resistive wall must be sufficiently close to plasma to achieve rotational stabilization of the mode but there is no lower limit on the wall position. Stabilizing rotation speeds are found somewhat smaller when compared to MHD results. In addition, for the present plasma configuration, the kinetic model predicts resistive wall mode stabilization only in one direction of toroidal rotation. In the opposite direction, a destabilizing effect is observed. This is in contrast to MHD where mode stabilization is symmetric with respect to the direction of the toroidal plasma rotation. [http://dx.doi.org/10.1063/1.3691653]

I. INTRODUCTION

The physics underlying the stabilization of the resistive wall mode (RWM) is an important issue in current fusion research. High beta plasmas in tokamaks require stabilization if the plasma beta is above the no-wall limit. Also, for long duration discharges in a reversed field pinch (RFP), the RWM is potentially disruptive. A comprehensive overview on existing modelling and experiments of the stabilization of the external kink and the resistive wall mode is given in Ref. 1. One of the first studies on the stabilization of external modes in tokamaks by resistive wall and the plasma rotation[2] addressed already the important question on the role of Landau damping of sound waves excited by plasma motion and propagating along the field lines. Different modifications of the ideal MHD equations have been suggested to account for this effect which is, however, kinetic in nature.[3,4] The stabilization mechanism with or without rational surfaces in the plasma are expected to be different.[5,6]

In recent studies of the interaction of low frequency resonant magnetic field perturbations (RMPs), it has been demonstrated that MHD theory has strong limitations in its applicability for modern tokamak parameter range.[7] Namely, the radial scale of resonant layers in plasma is comparable to the ion Larmor radius (FLR). Therefore, it is interesting to compare MHD results for various instabilities like kink modes and RWMs with results using the kinetic approach.

In Refs. 8 and 9, the linearized collisionless drift kinetic equation has been solved in toroidal geometry using guiding center variables to analyze plasma stability by means of quadratic forms obtained from the momentum balance equation. This approach allows to derive approximate analytical estimates of the plasma stability taking into account various effects like finite orbit widths and electrostatic potential perturbations. In Ref. 10, the magnetic drift kinetic damping of the resistive wall mode is studied based on the thermal particle resonance at magnetic drift and electron collision frequencies. Advanced mode damping beyond the ideal MHD description in connection with resistive wall mode control is discussed in Ref. 11.

In the present paper, a different straightforward method is used. It is based on a numerical solution of the full set of Maxwell equations in cylindrical geometry with the plasma current density taken from a kinetic model. We discuss briefly the approximations and basic steps of the method developed in Refs. 12 and 13. Following Mahajan-Chen,[14] action-angle variables are used to solve analytically the linearized Vlasov equation (no gyroaveraging) with a simplified one-dimensional Fokker-Planck collision operator (Ornstein-Uhlenbeck approximation). The background distribution function is taken in the form of an inhomogeneous drifting Maxwellian with parameters derived from the plasma and magnetic field profiles that satisfy the MHD equilibrium. Unperturbed particle orbits are used in the lowest order with respect to the thermal motion where all particle drifts related to the inhomogeneity of the background magnetic field are neglected and only the electric $\mathbf{E} \times \mathbf{B}$ drift is taken into account. A finite Larmor radius expansion is applied to evaluate the current density induced in the plasma by the rotating helical perturbations. In cylindrical geometry, the perturbation of the plasma current density depends on the electric field and also, due to the Larmor gyration effect, on the radial derivatives of the electric field. A particular finite Larmor radius expansion scheme (of arbitrary order) has been developed[13] such that the current density is covariant (up to

this order) with respect to Galilean transformations to a moving frame and the total power absorption for the case of a Boltzmann distribution of the background particles is non-negative. This is important in order not to create fake modes, i.e., artificial modes created by the expansion and not having a physical basis. Maxwell equations with displacement and plasma current densities together with the appropriate boundary conditions for an ideal or a resistive wall are solved numerically to find the eigenmodes existing in the system by a direct complex root search procedure.

The code KiLCA (kinetic linear cylindrical approximation) is a wave code based on the described kinetic model of the tokamak plasma in a periodic cylinder geometry.[12,13] The code has been successfully used[7,15] to study kinetic effects of the interaction of resonant magnetic perturbations and the plasma in particular near resonant magnetic surfaces. The present report describes results of the adaption of this code to study the resistive wall mode in a reversed field pinch plasma with a proper account of kinetic effects including Landau damping, transit-time magnetic pumping (TTMP) and particle collisions. In the general case, there are four different regions to be considered with increasing radius: the plasma region followed by a vacuum region followed by the ideal (or resistive) wall region followed by the outer vacuum region. The vacuum as well as the resistive wall region solutions are obtained analytically (Eq. (24)). Inside the plasma region, Maxwell's equations with the current density obtained from either the fluid model or the kinetic model are solved. The linear system of matching equations is assembled and solved to determine the superposition coefficients for the fundamental solutions in each region. Finite nonzero solutions that correspond to stable or unstable eigenmodes (depending on a sign of imaginary part of the eigenfrequency) are possible only when the determinant of the system is zero.

The results of the present study are to be compared to existing MHD results in particular to the results of the MHD calculations in Ref. 16. In this paper, the RFP configuration is based on the $\alpha - \theta_0$ model[17,18] with a constant density profile. The stability of the resistive wall mode is studied in a (periodic) cylindrical MHD model in which the effects of plasma pressure, compressibility, plasma inertia, longitudinal rotation, and parallel viscosity have been taken into account. The resistive wall is modelled in the above mentioned paper as well as in the present study with finite thickness and constant conductivity. In a recent paper,[19] the results of this model have been used for a comparison between cylindrical model and experimental observation on the study of resistive wall mode in reversed field pinch plasmas.

The paper is organized as follows. In Sec. II, the MHD equilibrium is discussed. In Sec. III, the eigenmode equations of ideal MHD including toroidal flows are described. In Sec. IV, the kinetic model is explained and in Sec. V analytic solutions for the resistive wall of finite thickness are discussed. Matching conditions are discussed in Sec. VI. A comparison of the results is done in Sec. VII and conclusions are given in Sec. VIII.

II. EQUILIBRIUM

An ideal MHD-equilibrium

$$\nabla p_0 = \frac{1}{c}\mathbf{j}_0 \times \mathbf{B}_0, \quad \nabla \times \mathbf{B}_0 = \frac{4\pi}{c}\mathbf{j}_0 \tag{1}$$

is considered in cylindrical geometry, i.e., $\mathbf{B}_0 = (0, B_{0\theta}(r), B_{0z}(r))$ is the equilibrium magnetic field, $p_0(r)$ is the equilibrium pressure, $\mathbf{j}_0(r)$ is the equilibrium current density, and c is the speed of light. The $\alpha-\Theta_0$ equilibrium model used in Ref. 16 is given by the following equations:

$$\frac{dB_{0z}}{dr} = -\mu B_{0\theta} - \frac{4\pi B_{0z}}{B_0^2}\frac{dp_0}{dr}, \tag{2}$$

$$\frac{1}{r}\frac{d}{dr}(rB_{0\theta}) = \mu B_{0z} - \frac{4\pi B_{0\theta}}{B_0^2}\frac{dp_0}{dr}, \tag{3}$$

$$\frac{dp_0}{dr} = -\chi\frac{r}{8\pi}\left(\frac{\mu B_0^2}{2B_{0z}} - \frac{B_{0z}}{r}\right)^2, \tag{4}$$

$$\mu = \frac{2}{a}\Theta_0\left[1 - \left(\frac{r}{a}\right)^{\alpha}\right]. \tag{5}$$

Here, $\mu(r)$ models the amount of parallel current density and a is the plasma radius. Equation (4) gives Suydam's necessary condition for stability when $\chi < 1$, and $q(0) = a/(R\Theta_0)$ is the on-axis safety factor.

Derived parameters describing this model are the poloidal beta β_p, the reversal parameter F, and the pinch parameter Θ,

$$\beta_p = \frac{8\pi}{B_{0\theta}^2(a)}\langle p_0\rangle = \frac{8\pi}{B_{0\theta}^2(a)}\frac{1}{\pi a^2}\int_0^a dr 2\pi r p_0(r), \tag{6}$$

$$F = \frac{B_{0z}(a)}{\langle B_{0z}\rangle}, \quad \Theta = \frac{B_{0\theta}(a)}{\langle B_{0z}\rangle}. \tag{7}$$

III. MHD MODELLING

After Fourier transformation in time, the linearized compressible ideal MHD equations with finite equilibrium flows $\mathbf{v}_0$ can be written with the help of the Lagrangian displacement vector ξ as (see, e.g., Ref. 20),

$$-\omega^2\rho_0\xi = \mathbf{F}(\xi), \tag{8}$$

$$\begin{aligned}\mathbf{F}(\xi) = {} & \nabla(\xi\cdot\nabla p_0 + \gamma p_0(\nabla\cdot\xi)) + \frac{1}{4\pi}\Big[(\nabla\times\mathbf{B}_0)\\ & \times\mathbf{B}_1 + (\nabla\times\mathbf{B}_1)\times\mathbf{B}_0\Big] + \nabla\cdot\Big[\rho_0\xi(\mathbf{v}_0\cdot\nabla)\mathbf{v}_0\\ & -\rho_0\mathbf{v}_0(\mathbf{v}_0\cdot\nabla)\xi\Big] + 2i\omega\rho_0(\mathbf{v}_0\cdot\nabla)\xi,\end{aligned} \tag{9}$$

where ω is the frequency, γ the adiabatic index, ρ_0 the equilibrium density, and $\mathbf{B}_1$ the magnetic field perturbation.

Introducing the variable

$$p^* = -\gamma p_0\nabla\cdot\xi - \xi\cdot\nabla p_0 + \frac{\mathbf{B}_0\cdot\mathbf{B}_1}{4\pi}, \tag{10}$$

in cylindrical geometry, the system reduces to two (complex) first order ordinary differential equations for $(r\xi_r)$ and p^* (see Refs. 21 and 22),

$$\frac{AS}{r}\frac{\mathrm{d}}{\mathrm{d}r}(r\xi_r) = C_{11}(r\xi_r) - C_{12}p^*,$$

$$AS\frac{\mathrm{d}}{\mathrm{d}r}p^* = C_{21}(r\xi_r) - C_{22}p^*, \tag{11}$$

with

$$A = \rho_0\tilde{\omega}^2 - \frac{F^2}{4\pi}, \quad S = \left(\frac{B_0^2}{4\pi} + \gamma p_0\right)\rho_0\tilde{\omega}^2 - \gamma p_0\frac{F^2}{4\pi}, \tag{12}$$

$$C_{11} = \rho_0\tilde{\omega}^2\frac{Q}{r^2} - 2m\frac{ST}{r^3}, \quad C_{12} = \rho_0^2\tilde{\omega}^4 - \left(k^2 + \frac{m^2}{r^2}\right)S, \tag{13}$$

$$C_{21} = \frac{AS}{r}C_4 - 4\frac{ST^2}{r^3} + \frac{Q^2}{r^3}, \quad C_{22} = rC_{11}, \tag{14}$$

$$T = \frac{FB_\theta}{4\pi} + \rho_0\tilde{\omega}V_\theta, \quad C_4 = A + r\frac{\mathrm{d}}{\mathrm{d}r}\left(\frac{B_\theta^2 - 4\pi\rho_0 V_\theta^2}{4\pi r^2}\right), \tag{15}$$

$$Q = \rho_0\tilde{\omega}^2\left(\frac{B_\theta^2}{4\pi} - \rho_0 v_\theta^2\right) + \frac{\rho_0}{4\pi}(B_\theta\tilde{\omega} + FV_\theta)^2. \tag{16}$$

Here, $F = k\cdot B_0$, $\tilde{\omega}$ is the Doppler shifted frequency

$$\tilde{\omega} = \omega - \frac{mV_\theta}{r} - kV_z, \tag{17}$$

m is the poloidal mode number and k the "toroidal" wave number, B_θ, B_z and V_θ, V_z are the respective components of background magnetic field and plasma velocity.

IV. KINETIC MODELLING

Following the linear kinetic model of a cylindrical inhomogeneous screw pinch plasma introduced in Ref. 12 and recently upgraded in Ref. 13, the wave fields $(\tilde{\mathbf{E}}, \tilde{\mathbf{B}})$ with frequency ω are obtained from Maxwell's equations,

$$\nabla\times\tilde{\mathbf{E}} = \frac{i\omega}{c}\tilde{\mathbf{B}}, \quad \nabla\times\tilde{\mathbf{B}} = -\frac{i\omega}{c}\tilde{\mathbf{E}} + \frac{4\pi}{c}\tilde{\mathbf{j}}, \tag{18}$$

solved numerically together with an appropriate set of boundary conditions.

The plasma response current density in Eq. (18) is evaluated as

$$\tilde{\mathbf{j}} = \sum_{\alpha=\{e,i\}} e_\alpha \int \mathrm{d}^3 p\mathbf{v}\tilde{f}_\alpha, \tag{19}$$

where e_α is a charge of species α, $\mathbf{v}$ is the velocity variable and the perturbed distribution function $\tilde{f}_\alpha$ satisfies the linearized Vlasov equation with Fokker-Planck type collision term (in the following, we omit index α for brevity)

$$\frac{\partial\tilde{f}}{\partial t} + \mathbf{v}\cdot\nabla\tilde{f} + e\left(-\nabla\Phi_0 + \frac{1}{c}\mathbf{v}\times\mathbf{B}_0\right)\cdot\frac{\partial\tilde{f}}{\partial\mathbf{p}} - \hat{L}_C\tilde{f} = -e\left(\tilde{\mathbf{E}} + \frac{1}{c}\mathbf{v}\times\tilde{\mathbf{B}}\right)\cdot\frac{\partial f_0}{\partial\mathbf{p}}. \tag{20}$$

Here, f_0 is the equilibrium distribution function consistent with plasma and magnetic field equilibrium profiles including the toroidal plasma rotation (the poloidal rotation is assumed to be zero), Φ_0 is the equilibrium electrostatic potential, and $\hat{L}_C$ models Coulomb collisions. For the description of particle collisions, we use a one-dimensional Fokker-Planck collision operator (Ornstein-Uhlenbeck approximation, see Ref. 23)

$$\hat{L}_c\tilde{f} = \frac{\partial}{\partial u_\parallel}D\left[\frac{\partial}{\partial u_\parallel} + \frac{u_\parallel - V_\parallel}{v_T^2}\right]\tilde{f}, \tag{21}$$

where $u_\parallel$ is a particle parallel velocity, D is a constant diffusion coefficient in velocity space, $v_T = \sqrt{T_0/m_0}$ is the thermal velocity, and $V_\parallel$ is a bulk parallel velocity of the given species. Following the procedure outlined in Mahajan-Chen,[14] Eq. (20) is solved analytically in action-angle variables.[12,13]

Generally, the current density Eq. (19) is an integral functional of the perturbation field and, due to finite FLR effect, it remains to be so even in cylindrical geometry $\mathbf{x} = (r, \vartheta, z)$ where Fourier analysis over poloidal and toroidal angles transforms the integral nonlocality with respect to these angles into an algebraic dependence.

We apply a finite Larmor radius expansion procedure to evaluate the perturbation of the current density induced in the plasma by a single harmonic perturbation of the vector potential with the frequency ω

$$\tilde{\mathbf{A}}(\mathbf{x}, t) = \mathrm{Re}\tilde{\mathbf{A}}(r)\mathrm{e}^{ik_\vartheta\vartheta + ik_z z - i\omega t}, \tag{22}$$

where $k_\vartheta = m$, $k_z = n/R$, and (m, n) are poloidal and toroidal numbers of the helical perturbation. For the perturbation field, we use the radiation gauge $\tilde{\Phi} = 0$ such that the electric field is defined solely by the vector potential $\tilde{\mathbf{E}} = \frac{i\omega}{c}\tilde{\mathbf{A}}$. Static perturbations with $\omega = 0$ can be treated by transforming to a moving frame where the perturbation frequency is finite.

Due to the special finite Larmor radius expansion scheme (of arbitrary order), the following fundamental properties of the exact current density are preserved: (1) covariance with respect to Galilean transformations to a moving frame (approximate) and (2) nonnegative total power absorption for the case of a Boltzmann distribution of the background particles (no fake modes).

For the analytical evaluation of the current density, the unperturbed particle orbits are used in lowest order with respect to the thermal motion. All particle drifts related to the inhomogeneity of the background magnetic field are neglected and only the electric $\mathbf{E}\times\mathbf{B}$ drift is taken into account.

In cylindrical geometry, contravariant components of the perturbation of plasma current density $\tilde{j}^k_{(N)}$ depend on covariant components of the electric field $\tilde{E}_j$ and, due to the Larmor gyration effect, also on the derivatives of the electric field,

$$\tilde{j}^{k}_{(N)} = \frac{1}{r}\sum_{n,n'=0}^{N}(-)^{n}\frac{\partial^{n}}{\partial r^{n}}\left(r\sigma^{kj}_{nn'}(r,\mathbf{k})\frac{\partial^{n'}}{\partial r^{n'}}\tilde{E}_{j}\right). \quad (23)$$

Here, N is the order of Larmor radius expansion and the conductivity matrices $\sigma^{kj}_{nn'}$ are defined as integrals over the particle actions space.

V. VACUUM AND RESISTIVE WALL REGIONS

The solutions of Maxwell's equations for cylinder geometry and constant conductivity σ can be expressed like the corresponding vacuum solutions by a linear combination of modified Bessel functions

$$C_1 I_m(\alpha^* r) + C_2 K_m(\alpha^* r) \quad (24)$$

with C_1 and C_2 constant coefficients, and derivatives of this combination where

$$(\alpha^*)^2 = k^2 - \frac{\omega\omega^*}{c^2}, \quad (25)$$

$$\omega^* = \omega + 4\pi i\sigma. \quad (26)$$

VI. MATCHING CONDITIONS

There are four different regions to be considered with increasing radius: the plasma region followed by a vacuum region followed by the ideal (or resistive) wall region followed by the outer vacuum region. The vacuum as well as the resistive wall region solutions is obtained analytically (24). Inside the plasma region, Maxwell's equations with the current density obtained from either the fluid model or the kinetic model are solved. Fourier transforming with respect to time as well as poloidal and toroidal angles yields a set of ordinary differential equations. The various modes have very different spatial scales and, therefore, an appropriate solver for the stiff boundary value problem is used.

The linear system of matching equations is assembled and solved to determine the superposition coefficients for the fundamental solutions in each region. For each type of interface (e.g., kinetic plasma—vacuum or MHD plasma—vacuum, wall—vacuum, etc.), an appropriate set of matching conditions on the wave field components is applied. For an arbitrary complex mode frequency ω, the system determinant $\det(\omega)$ is nonzero and, therefore, the solution (all superposition coefficients) is zero since there are no sources (rhs equals zero) in the system. Finite nonzero solutions that correspond to stable or unstable eigenmodes (depending on a sign of imaginary part of the eigenfrequency) are possible only when the determinant is zero. A complex root solver is used to find all roots of the dispersion equation $\det(\omega) = 0$ numerically.

VII. COMPARISON AND DISCUSSION OF THE RESULTS

In the kinetic model, there exist several additional plasma parameters which are not present in the concurrent MHD model. In particular, we can choose both the ion and the electron temperature profiles as well as different particle collision frequencies. Depending on the values of these "free" parameters, better or worse agreement with MHD results can be achieved. In the present work, we have chosen values for plasma parameters representative for typical experimental setups. In addition, since kink and resistive wall mode properties are very sensitive to the plasma profiles, it seems not to be appropriate to make direct predictions about experimental situations. For this purpose, a detailed simulation with a complete set of experimental settings is needed.

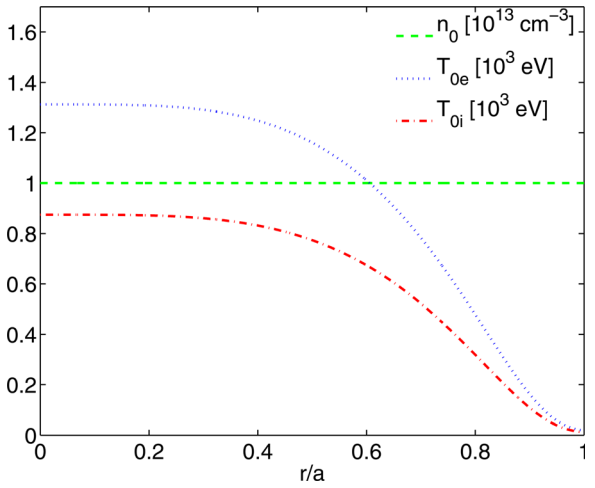

FIG. 1. (Color online) Background profiles for density n_0, electron temperature T_{0e}, and ion temperature T_{0i}.

Figure 1 shows the profiles of density and temperatures, Figure 2 the profiles of safety factor, poloidal, and toroidal magnetic fields used in the calculations. These profiles correspond to parameter values $\alpha = 8.16$, $\Theta_0 = 1.5$, $\chi = 1$, resulting in $F = -0.59$, $\beta_p = 0.081$, and $\Theta = 1.93$.

For the dimensional quantities shown in Figures 1 and 2 and taking $a = 50$ cm, one gets

$$\omega_A = \frac{V_A}{a} = \frac{B_{0\theta}(a)/\sqrt{4\pi\rho}}{a} = 2.34\times 10^{6}\,\mathrm{s}^{-1}, \quad (27)$$

$$\tau_A = \frac{1}{\omega_A} = 4.27\times 10^{-7}\,\mathrm{s} \quad (28)$$

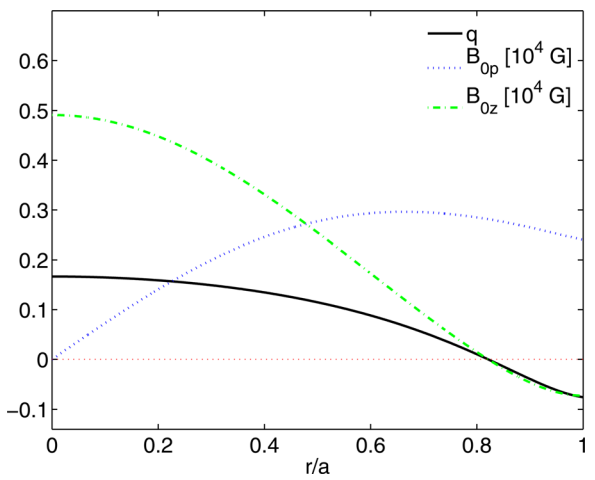

FIG. 2. (Color online) Background profiles for safety factor q, poloidal magnetic field B_{0p}, and toroidal magnetic field B_{0z}.

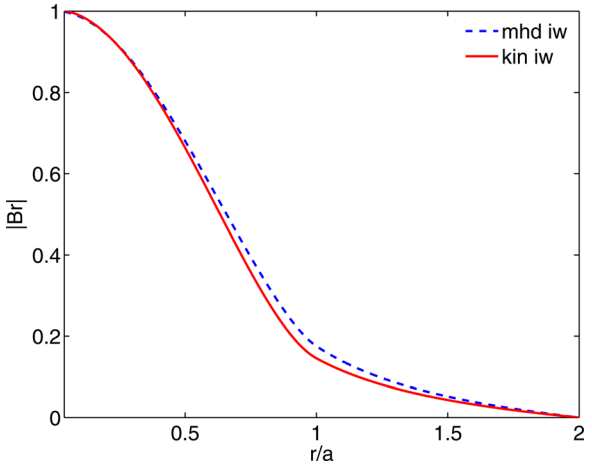

FIG. 3. (Color online) Profiles of the modulus of the radial magnetic field $|B_r|$ for the ideal wall at $b/a = 2$ (ideal kink mode) without toroidal plasma rotation. Toroidal and poloidal ode numbers are $n = 3$ and $m = 1$ such that the toroidal wave number normalized to the small radius a is $ka = 0.75$. Blue (dashed)—MHD model and red (solid)—kinetic model.

as the typical Alfvén rotation frequency ω_A and the ideal time scale τ_A. The resistive wall time scale τ_w for wall position $b = 50$ cm, wall thickness $h = 5$ cm, and wall conductivity $\sigma = 4.5 \times 10^{14}\ \mathrm{s}^{-1}$ is then

$$\tau_w = \frac{4\pi b h \sigma}{c^2} = 0.0016\,\mathrm{s} = 3.7 \times 10^3\,\tau_A. \qquad (29)$$

Toroidal and poloidal mode numbers are chosen $n = 3$, $m = 1$, i.e., $k = n/R$. For a big radius $R = 200$ cm, the values agree with values in Ref. 16, namely $ka = 0.75$.

For the ideal wall positioned at $b/a = 2$, the radial magnetic field $|B_r|$ for the kink instability is shown in Figure 3. Figure 4 shows the normalized $|B_r|$ profile for modes with the resistive wall positioned at $b/a = 1.4$. In this case, two kinetic roots have been found whose growth rates are shown

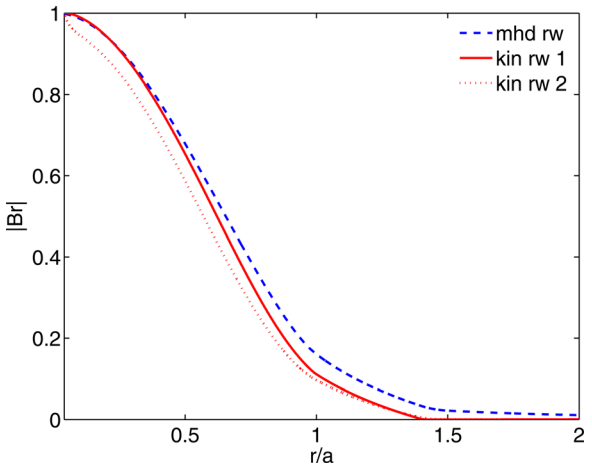

FIG. 4. (Color online) Profiles of the modulus of the radial magnetic field $|B_r|$ for the resistive wall at $b/a = 1.4$ (resistive wall mode) without toroidal plasma rotation. Mode numbers are the same as in Figure 3. The ratio of resistive to Alfvénic (ideal) time scale is $\tau_w/\tau_A = 3.7 \times 10^3$. Blue (dashed)—MHD model and red (solid and dotted)—kinetic model.

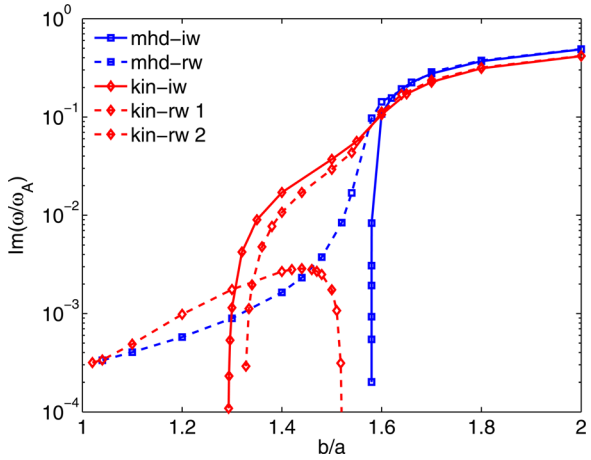

FIG. 5. (Color online) Normalized growth rates without any plasma rotation for the "kink" and the "resistive" mode plotted over the ideal/resistive wall position. Mode numbers are $m = 1$ and $n = 3$. The resistive time scale is $\tau_w/\tau_A = 3.7 \times 10^3$. Solid lines (square—MHD and diamond—kinetic) for the ideal wall and dashed and dot-dashed lines for the resistive wall. The kinetic model shows the slightly modified ideal kink mode for a resistive wall labeled kin-rw 1 and a new branch for $1.35 < b/a < 1.52$, the resistive mode labeled kin-rw 2.

in Figure 5 below. The $|B_r|$ profiles for the MHD and the kinetic model are seen in good qualitative agreement.

Figure 5 shows the normalized growth rates of the ideal wall mode and the resistive wall mode as a function of the wall position. The MHD result is the same as shown in Figures 5 and 6 of Ref. 16. The kinetic description of the kink type mode (ideal wall) shows a slightly smaller growth rate for $1.6 < b/a < 2$. More remarkably, one can observe a significant smaller wall minor radius for mode stabilization about $b/a \approx 1.3$ compared to $b/a \approx 1.6$ for MHD. Nevertheless, the mode can be still stabilized by an ideal wall close enough to the plasma.

If the wall is resistive, the resistive wall mode appears. In the MHD case, there exists now a mode even for values of $b/a < 1.6$ with growth rates three orders of magnitude smaller, i.e., on the resistive time scale. In the kinetic case, the situation is somewhat different. For values above the

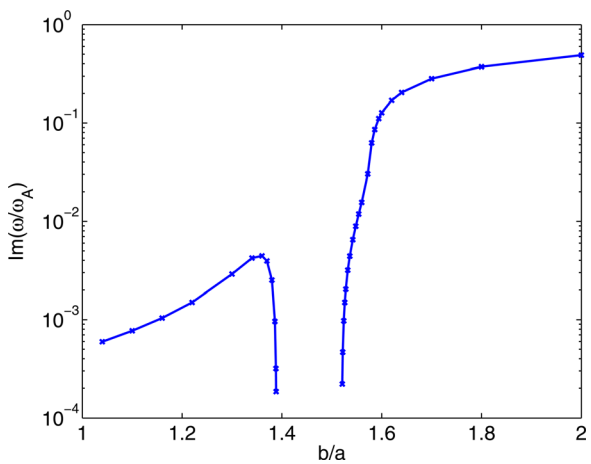

FIG. 6. (Color online) The stability window $1.4 < b/a < 1.55$ for the RWM predicted by the MHD model with toroidal rotation velocity $V_z/V_A = 0.5$.

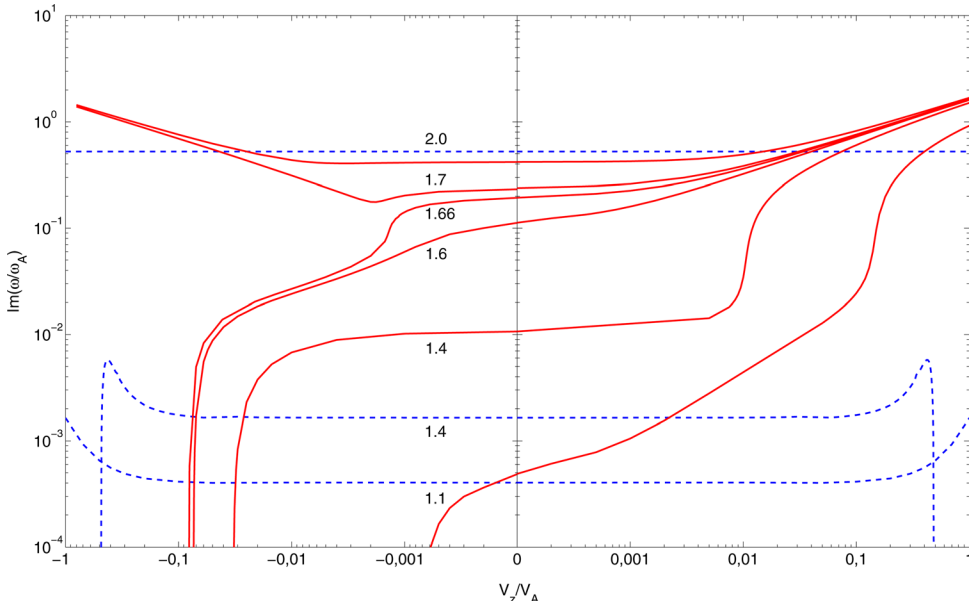

FIG. 7. (Color online) Normalized growth rates of the RWM for different wall positions $1.1 < b/a < 2$ as a function of the normalized toroidal plasma velocity V_z/V_A. Solid curve labeled $b/a = 1.1$ corresponds to kin-rw 2, all other solid curves correspond to kin-rw 1 as shown for zero plasma rotation in Figure 5. Mode numbers are $m = 1$ and $n = 3$. The resistive time scale is $\tau_w/\tau_A = 3.7 \times 10^3$. Dashed lines—MHD model and solid lines—kinetic model. Left—toroidal plasma rotation against and right—toroidal plasma rotation with the toroidal plasma current.

ideal stabilization values of $b/a < 1.3$, there is, similar to MHD, not much difference to the ideal wall. For small values of the wall position, $1 < b/a < 1.52$, there appears now a new mode, the kinetic resistive wall mode. Again, the growths rates found by the kinetic model are in good qualitative agreement with the MHD results.

The next point to be addressed is the role of mode stabilization by toroidal rotation of the plasma. For this case, MHD predicts a stability window[16] which is shown in Figure 6. Figure 7 shows the growth rates over toroidal rotation for different positions of the resistive wall. On the left, the results for negative V_z are shown, on the right, the results for positive V_z (plasma current is positive). The first thing one can realize is that for MHD, the mode stabilization is symmetric with respect to the sign of V_z. This can be also seen from the formulae in the MHD modelling section if the poloidal velocity is zero. In contrast, kinetic modelling shows stabilization only for $V_z < 0$ values, whereas for $V_z > 0$, the growth rates slightly increase instead. In the kinetic model, the toroidal plasma rotation velocity influences the background electric field and the parallel bulk velocity parameter of the ion and electron background distribution functions. In the expressions that define those quantities, there is no symmetry that may lead to an asymmetric behavior of the instability growth rates with respect to direction of toroidal plasma rotation.

Another difference is seen for wall position $b/a = 1.1$. MHD predicts instability whereas kinetic theory does not. That means instead of the stability window shown in Figure 6, in the kinetic model, there is an upper threshold, $b/a \approx 1.68$ for the wall position only: if the wall is too far away the RWM is not stabilized even for large toroidal rotation velocities. In MHD, there is also a lower threshold, $b/a \approx 1.4$,

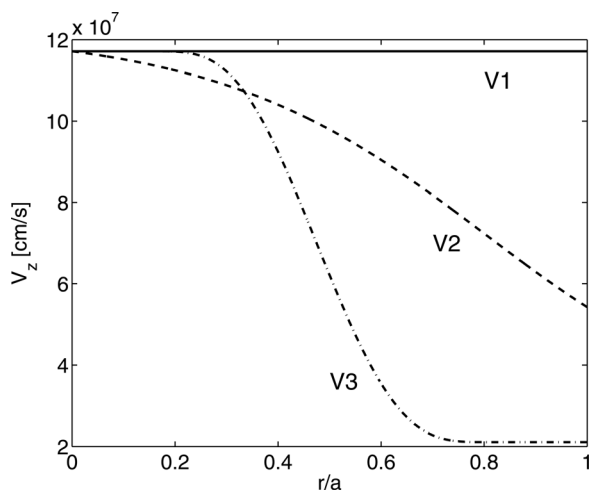

FIG. 8. Three different profiles for the toroidal plasma rotation velocity used in the calculations for Figure 9.

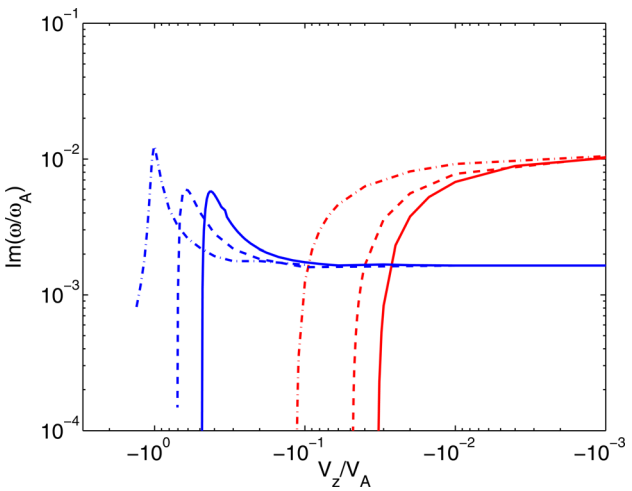

FIG. 9. (Color online) Normalized growth rates for the RWM at $b/a = 1.4$ as a function of the normalized toroidal plasma velocity V_z/V_A for different profiles of the toroidal background plasma velocity shown in Figure 8: V1 solid, V2 dashed, and V3 dashed-dotted. Left curves—MHD model and right curves—kinetic model.

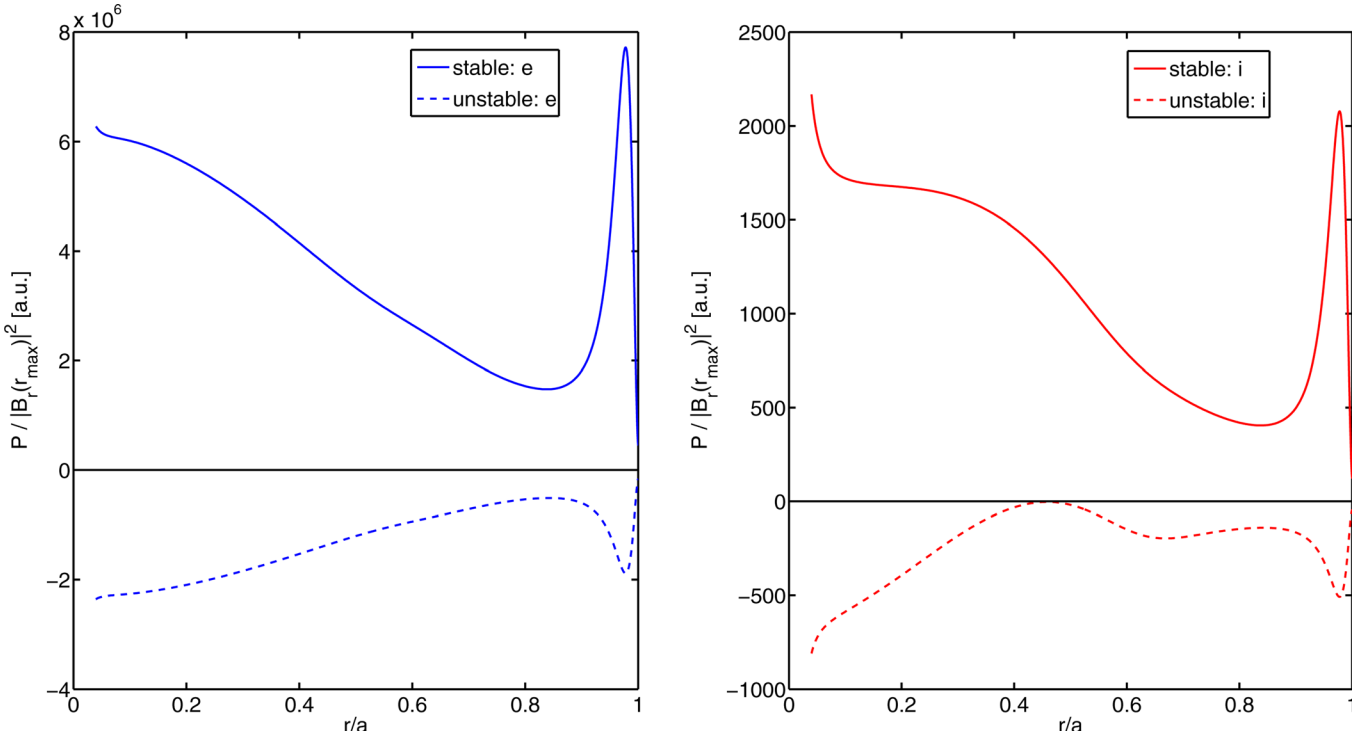

FIG. 10. (Color online) Power densities (normalized to the maximum value of $|B_r|^2$) dissipated to electrons (left) and to ions (right) for a stable ($V_z/V_A = -0.04$) and an unstable ($V_z/V_A = -0.03$) RWM and resistive wall position at $b/a = 1.4$.

and the RWM is not stabilized for the resistive wall too close to the plasma.

For the case $b/a = 1.4$, one concludes from Figure 7 that in the kinetic model, toroidal velocities of about 3% of the Alfvén velocity stabilize the RWM whereas in the MHD model this value is about 30%. Small rotation speeds of a few percent of the Alfvén velocity have also been found in Ref. 24 to be sufficient for stabilization of resistive wall modes in ITER by toroidal rotation. For a better understanding, three different rotation profiles shown in Figure 8 have been tested. The results in Figure 9 show that for smaller rotations speeds at the plasma edge, the stabilization value for the case $b/a = 1.4$ increases up to 10% of the Alfvén speed. It is concluded that a high enough plasma rotation at the edge is important for stabilization, whereas differential rotation seems to have no significant impact.

Also, different density profiles with smooth behavior at the plasma edge have been tested. But, this did not lead to any significant changes of the results.

An important question is where the energy goes during RWM stabilization. For the frequency range typical to RWM, only Cerenkov resonance will contribute to the interaction between the electromagnetic field and particles that in the present cylindrical model are all passing particles. However, it is most likely that magnetic perturbation along the magnetic field lines acting via the grad B force on the particles will add up to the parallel electric perturbation field and thus to the work of the electric field on the parallel current. The relative impact of different sorts of particles on the mode stability can be analyzed by looking at the electromagnetic power dissipated to the respective species. If total power dissipated to the electrons and ions together is positive, the mode will damp. Vice versa, if it is negative, the mode will obtain energy from the plasma particles and will grow, i.e., become unstable.

In Figure 10 shown are power densities dissipated to electrons and ions for the case of a stable (plasma rotates with $V_z = -0.04V_A$) and an unstable ($V_z = -0.03V_A$) RWM mode with resistive wall position at $b/a = 1.4$ cm. While the power densities dissipated on both species have the same sign (positive for the stable and negative for the unstable mode), it is the electrons which are responsible for the RWM stability since the energy dissipated to the ions is three orders of magnitude less.

VIII. CONCLUSIONS

Resistive wall mode stabilization has been investigated in a RFP plasma configuration within the kinetic model of a cylindrical plasma which accounts for Landau damping, TTMP, and Coulomb collisions. For this purpose, the code KiLCA, originally developed for treating the plasma response due to external RMPs, has been adapted to deal with stable and unstable global eigenmodes that are determined by plasma, vacuum, and vessel parameters. This code can now be used to study resistive wall modes in reversed field pinch and tokamak plasmas.

The external kink mode stabilized in ideal MHD by an ideal wall has been found also in the kinetic description with comparable growth rates. The wall position for complete stabilization of the ideal mode is less than predicted by MHD.

A resistive wall mode with growth rate on the resistive time scale is also seen in the kinetic description. In analogy to MHD, this mode was found to be stabilized by toroidal plasma

motion. However, stabilization in the kinetic modelling is sensitive to the direction of the rotation and, in the present case, only negative V_z values have led to mode stabilization. Stabilizing rotation velocities are found somewhat smaller when compared to MHD. Finally, we did not see the complete stabilizing window predicted by MHD, which means we did not find instability for very close positions of the resistive wall.

In the kinetic model proposed in the present paper, mode damping is essentially associated with dissipation of wave energy to passing electrons. Dissipation is intermediated by Landau damping, TTMP, and collisions. Estimates show that within the presented model, Landau damping contributes at least one order of magnitude more than TTMP to wave damping. In particular, collisionless Landau damping is seen to be the prime mechanism, whereas TTMP and collisions play a minor role in mode damping.

ACKNOWLEDGMENTS

This work, supported in part by the European Commission under the contract of Associations between EURATOM and the Austrian Academy of Sciences, was carried out within the framework of the European Fusion Development Agreement. The views and opinions expressed herein do not necessarily reflect those of the European Commission. Additional funding is provided by the Austrian Science Foundation, FWF, under Contract No. P19889-N16.

[1]M. S. Chu and M. Okabayashi, Plasma Phys. Controlled Fusion **52**, 123001 (2010).
[2]A. Bondenson and D. J. Ward, Phys. Rev. Lett. **72**, 2709 (1994).
[3]R. Betti and J. P. Freidberg, Phys. Rev. Lett. **74**, 2949 (1995).
[4]R. Fitzpatrick and A. Y. Aydemir, Nucl. Fusion **36**, 11 (1996).
[5]J. M. Finn, Phys. Plasmas **2**, 3782 (1995).
[6]A. Bondenson and H. X. Xie, Phys. Plasmas **4**, 2081 (1997).
[7]M. F. Heyn, I. B. Ivanov, S. V. Kasilov, and W. Kernbichler, Nucl. Fusion **48**, 024005 (2008).
[8]T. M. Antonsen, Jr., and Y. C. Lee, Phys. Fluids **25**, 132 (1982).
[9]F. Porcelli, R. Stankiewicz, and W. Kerner, Phys. Plasmas **1**, 470 (1994).
[10]Y. Q. Liu, M. S. Chu, C. G. Gimblett, and R. J. Hastie, Phys. Plasmas **15**, 092505 (2008).
[11]Y. Q. Liu, M. S. Chu, W. F. Guo, F. Villone, R. Albanese, G. Ambrosino, M. Baruzzo, T. Bolzonella, I. T. Chapman, A. M. Garofalo, C. G. Gimblett, R. J. Hastie, T. C. Hender, G. L. Jackson, R. J. La Haye, M. J. Lanctot, Y. In, G. Marchiori, M. Okabayashi, R. Paccagnella, M. F. Palumbo, A. Pironti, H. Reimerdes, G. Rubinacci, A. Soppelsa, E. J. Strait, S. Ventre, and D. Yadkin, Plamsa Phys. Controlled Fusion **52**, 104002 (2010).
[12]M. F. Heyn, I. B. Ivanov, S. V. Kasilov, and W. Kernbichler, Nucl. Fusion **46**, S159 (2006).
[13]I. B. Ivanov, M. F. Heyn, S. V. Kasilov, and W. Kernbichler, Phys. Plasmas **18**, 022501 (2011).
[14]S. M. Mahajan and C. Y. Chen, Phys. Fluids **28**, 3538 (1985).
[15]I. B. Ivanov, S. V. Kasilov, W. Kernbichler, and M. Heyn, JETP Lett. **86**, 364 (2007).
[16]S. C. Guo, J. P. Freidberg, and R. Nachtrieb, Phys. Plasmas **6**, 3868 (1999).
[17]V. Antoni, D. Merlin, S. Ortolani, and R. Paccagnella, Nucl. Fusion **26**, 1711 (1986).
[18]D. Merlin, S. Ortolani, R. Paccagnella, and M. Scapin, Nucl. Fusion **29**, 1153 (1989).
[19]Z. R. Wang, S. C. Guo, L. Shi, T. Bolzonella, M. Baruzzo, and X. G. Wang, Phys. Plasmas **17**, 052501 (2010).
[20]J. Freidberg, *Ideal Magnetohydrodynamics* (Plenum, New York, 1987).
[21]A. Bondenson, R. Iacono, and A. Bhattacharjee, Phys. Fluids **30**, 2167 (1987).
[22]T. D. Arber and D. F. Howell, Phys. Plasmas **3**, 554 (1996).
[23]N. G. van Kampen, *Stochastic Processes in Physics and Chemistry* (Elsevier, Amsterdam, 1992).
[24]Y. Liu, A. Bondenson, Y. Gribov, and A. Polevi, Nucl. Fusion **44**, 232 (2004).